Building Tomorrow's Society
*Bâtir la Société de Demain*

Fredericton, Canada
June 13 – June 16, 2018/ *Juin 13 – Juin 16, 2018*

# NUMERICAL 3-D FEM OF FINGER-JOINT CONFIGURATION FOR SPRUCE LUMBER

Said, M. Essam[1, 4], Hussein, Amgad[2] and Lye, Leonard M.[3]
[1, 2, 3] Faculty of Engineering, Civil Department, Memorial University of Newfoundland, Canada
[4] meaas2@mun.ca

**Abstract:** The objective of this study is to create a numerical 3-D finite element model using Abaqus to simulate structural finger-joined spruce wood lumber. Finger joint (FJ) is the technique of joining the ends of two pieces of wood to make a longer piece. The created numerical model expressed here is based on cohesive zone model using traction-separation law to model the interface between the two adherent parts. To create a finite element model to simulate finger-joined lumber, properties of both wood and glue need to be specified. Spruce wood properties comprised of 3-young's moduli, 6-poisson's ratios, and 3-shear moduli. The glue-line properties are the initial stiffness, damage initiation (described by the interface strength), and damage evolution (described by the interface fracture toughness) in a Mixed-Mode behaviour. The model could be used to evaluate the structural performance and the configuration of FJ elements. A total of six-specimens of actual dry dimensions 38 x 89 x 1000 $mm^3$ were tested in the laboratory to measure the deflection at mid-span in order to validate the numerical FEM. Three of the specimens have no FJ while the other three have a FJ at the mid-span. The FJ length was 28.27 mm, the pitch was 6.33 mm, and finger-tip width (tip thickness) was 0.76 mm. FJs were assembled with a one face structural melamine-urea-formaldehyde adhesive of constitutive thickness $T_0 = 0.3mm$. The results showed that the load-displacement curves are in close agreement between the experimental and numerical model data which seem to validate the developed model for adhesive properties with the spruce adherent used.

**Keywords**: 3-D Finite Element Model, Abaqus, Finger-joint, Cohesive Zone Models.

## 1 INTRODUCTION

The modelling of finger-joint (FJ) using 3-D finite elements analysis considered here is one avenue which will lead to the improved exploitation of timber resources. The Finger jointing (FJ) is a technique that involves the joining of two pieces of lumber together by gluing two interlocking ends, hence reducing wastage of valuable lumber. This technique makes the unused and normally wasted short wood pieces into valuable lumber elements. FJ can extend the scraps by joining them together end to end that will benefit both nature and humans. Finger-joined lumber is an Engineered Wood Product (EWP) which contributes to export revenue and the economy of Canada. EWPs are green construction materials which contribute in decreasing the global warming through timber buildings that could help to cool the planet (Tollefson, 2017). In addition, EWPs have the capability of being reused and recycled. There are five steps which should be considered when manufacturing engineered finger-joined wood products: material selection, FJ profile, adhesive used, assembly procedure, and adhesive curing. These steps have variations according to the factory conditions and system used (Jokerst, 1981). FJ can be classified as structural or non-structural depending on the intended use and on its profile. Structural FJs are longer with sharper tips unlike the non-structural FJs which are short with blunt tips.

Finger-joints (FJ) with different wood species have been studied in the literature. The structural behaviour of FJ depends on: wood type, adhesive type, the compatibility between adhesive, wood, and FJ profile. C. Sandhaas, and J.W.G. Van de Kuilen (2013) developed a numerical 3-D finite elements material model for wood based on the concepts of Continuum Damage Mechanics (CDM). The determination of the necessary mechanical properties was considered the major point in the model, whereas both model performance and prediction capacity was dependent on these properties. A material subroutine was created containing the developed finite element model. Eight stress-based failure criteria (or damage initiation functions) were derived to formulate piecewise defined failure surfaces. The eight stress-based failures criteria were defined by the material strengths in tension, compression, and shear (longitudinal and tangential) in parallel and perpendicular directions. The damage development of wood was controlled by nine damage variables (or nine-stiffness parameters). Three different wood species (spruce, beech, azobé) were carried out using embedment tests whose results were compared to modelling outcomes. The results showed a close agreement between the experimental and numerical load-displacement curves data. Wood is highly anisotropic material, hence, the study also showed ductile behaviour in compression and brittle behaviour in tension and shear, where both failure modes can occur simultaneously. Eventually, the constitutive model was used to predict the results of embedment tests to assess the load carrying capacity and mechanical behaviour of timber joints (Sandhaas and Van de Kuilen, 2013). Another study by V.D. Tran, M. Oudjene, and P.J. Meausoone (2014) presented experimental and numerical 2-D finite element data on the mechanical behavior of finger-joined timber beech wood. Numerical simulations based on the Cohesive Zone Model (CZM) of Abaqus FEM software were developed to simulate the progressive failure. Two and three-layers glued beams with and without FJs from laminations of 42 mm thickness were constructed. The FJ lengths were 22 mm, the pitch was 6 mm, and finger-tip width (tip thickness) was 1 mm. FJs were assembled with a one face glue of melamine urea formaldehyde (MUF) adhesive. The bi-linear traction separation law was used to simulate the progressive failure of the FJ. The created numerical model assumes initially linear elastic behavior followed by the damage initiation and the damage evolution. The results showed that the glued-solid beech timber beams without FJ behaved better and present greater MOR than beams with FJ. Inspection of failure modes revealed that beams with FJ in the maximum tension zone showed premature failure, which propagated by steps: it took place, first, at the FJ and then propagated to the inter-layer bond-line. Therefore, from the obtained results, the actual FJ was the weak links of glued-solid beech timber beams. Eventually, the constitutive finite element model could predict the non-linear behavior of timber beech material with brittle failure in shear, tension parallel and perpendicular to grain. The model could also predict the damage and crack propagation across the glue-lines with in FJ (Tran, Oudjene and Meausoone, 2014). A different study from S. Fortino, et al. (2012) presented a numerical 3-D finite element model for the simulation of the cohesive short-term crack propagation (Mode I) in timber structures. The Mode I crack growth in solid wood and across the bond-lines of glulam was modelled using the cohesive elements of Abaqus FEA and exponential damage laws. To simulate the cohesive crack growth in wood, a damage initiation criterion of maximum stress, a damage evolution of displacement with exponential softening, and a traction type mixed mode ratio were used. Experimental work of modified double cantilever beam (DCB) specimens was established. Two types of modified DCB glulam specimens with two different adhesives, hyper-branched polyurethane (HBPU) and melamine urea formaldehyde adhesives (MUF), were tested. The load-displacement curves were then calculated for both experimentally and numerically to compare the data. The results showed a close agreement between the experimental and numerical load-displacement curves data with the notice of some influence of different adhesives on fracture response of the tested specimens. Eventually, The numerical modeling was suitable for solid wood and glulam cracked specimens under short-term fracture tests where the crack propagated in a known direction (Fortino *et al.*, 2012).

In this study, the aim was to create a numerical 3-D finite element model using Abaqus to simulate structural finger-joined spruce wood lumber. The created numerical model was based on cohesive zone model using traction-separation law to model the interface between the two adherent parts. The numerical load-displacement curve were then calculated to be compared with the experimental curve to validate the developed model for adhesive properties with the spruce adherent used. Hence, this research is a significant contribution to the development of FJs techniques with great potential for wider structural applications.

## 2 NUMERICAL FE MODEL APPROACH

Finger-joined lumber is a composite material which consists of timber and glue. The determination of the mechanical properties for both materials are essential to develop a finite element model (FEM), so that the model simulates the true structural behaviour of the element. The timber (adherent) properties can be determined from standard tests according to NLGA-SPS-1 for finger-joined structural lumber (NLGA-SPS-1, 2014). Also, the glue-line's properties (adhesive) can be determined from two tests for mode I (pure tension) and mode II (pure shear). For glue-line properties in mode I, the Double Cantilever Beam (DCB) test can be set up similar to that presented in (Fortino *et al.*, 2012; Tran, Oudjene and Meausoone, 2014; Tran, Oudjene and Méausoone, 2015). Subsequently, the pure shear test can be set up for mode II similar to that presented in (Tran, Oudjene and Meausoone, 2014; Tran, Oudjene and Méausoone, 2015). According to Tran et al (2014) the FJ fracture process is often caused by a combination of the two modes together in Mixed-Mode behaviour as shown in Figure 1 (Tran, Oudjene and Meausoone, 2014; Tran, Oudjene and Méausoone, 2015).

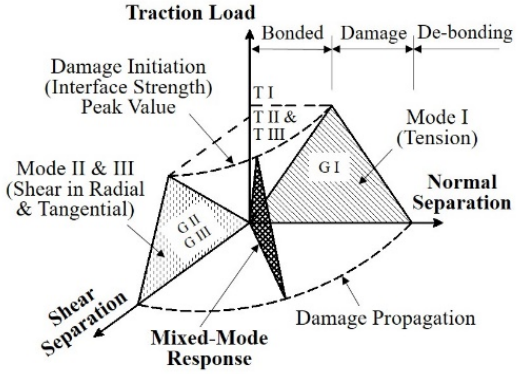


Figure 1 Schematic for Mixed-Mode Response

Both tension and shear modes may be combined. For instance, splitting parallel to longitudinal-radial-plane can be caused by tension perpendicular-to-grain (mode I), shear (mode II) or a combination of both (mixed mode) (Sandhaas and Van de Kuilen, 2013).

### 2.1 Modeling Approach of the timber

Wood could be considered as an orthotropic material defined by three directions: longitudinal (L), radial (R), and tangential (T) (see Figure 2). The model depends on the loading conditions and the environmental effects such as moisture and temperature variations. For instance, short-term loading condition and small variations in moisture content may be sufficient for employing linear elastic model. In other cases, plasticity and fracturing must be considered under long-term loading condition such as creep effects (Holmberg, Persson and Petersson, 1999; Dassault Systèmes Simulia, 2013; Sandhaas and Van de Kuilen, 2013).

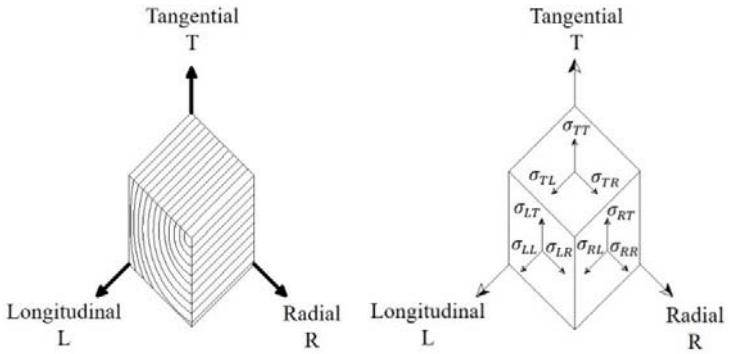


Figure 2 Stress Components and Material directions

Orthotropic elastic material model can be assumed for the timber material. Linear elasticity in an orthotropic material can be defined by giving nine-independent elastic stiffness parameters (or nine-damage variables) (Dassault Systèmes Simulia, 2013; Sandhaas and Van de Kuilen, 2013). Hooke's generalized law for an orthotropic material like wood can be written as follow:

$$\sigma_{ij} = D_{ijkl}\,\varepsilon_{kl}$$

where, $D_{ijkl}$ is the material stiffness parameters which can be defined by the engineering constants for an orthotropic material. The 9-elastic stiffness parameters $D_{ijkl}$ in orthotropic constitutive equations are comprised of 3-young's moduli $(\mathrm{E}_L, \mathrm{E}_R, \mathrm{E}_T)$, 6-poisson's ratios $(\nu_{LR}, \nu_{LT}, \nu_{RT}, \nu_{TR}, \nu_{RL}, \nu_{TL})$, and 3-shear moduli $(G_{LR}, G_{RT}, G_{TL})$ as follows:

$$\begin{Bmatrix} \sigma_{LL} \\ \sigma_{RR} \\ \sigma_{TT} \\ \sigma_{LR} \\ \sigma_{LT} \\ \sigma_{RT} \end{Bmatrix} = \begin{bmatrix} D_{LLLL} & D_{LLRR} & D_{LLTT} & 0 & 0 & 0 \\ D_{RRLL} & D_{RRRR} & D_{RRTT} & 0 & 0 & 0 \\ D_{TTLL} & D_{TTRR} & D_{TTTT} & 0 & 0 & 0 \\ 0 & 0 & 0 & D_{LRLR} & 0 & 0 \\ 0 & 0 & 0 & 0 & D_{LTLT} & 0 \\ 0 & 0 & 0 & 0 & 0 & D_{RTRT} \end{bmatrix} \begin{Bmatrix} \varepsilon_{LL} \\ \varepsilon_{RR} \\ \varepsilon_{TT} \\ \gamma_{LR} \\ \gamma_{LT} \\ \gamma_{RT} \end{Bmatrix}$$

where, $D_{ijkl} = \Gamma \cdot \begin{bmatrix} \mathrm{E}_L(1-\nu_{RT}\nu_{TR}) & \mathrm{E}_L(\nu_{RL}-\nu_{TL}\nu_{RT}) & \mathrm{E}_L(\nu_{TL}-\nu_{RL}\nu_{TR}) & 0 & 0 & 0 \\ \mathrm{E}_R(\nu_{LR}-\nu_{TR}\nu_{LT}) & \mathrm{E}_R(1-\nu_{LT}\nu_{TL}) & \mathrm{E}_R(\nu_{TR}-\nu_{LR}\nu_{TL}) & 0 & 0 & 0 \\ \mathrm{E}_T(\nu_{LT}-\nu_{LR}\nu_{RT}) & \mathrm{E}_T(\nu_{RT}-\nu_{RL}\nu_{LT}) & \mathrm{E}_T(1-\nu_{LR}\nu_{RL}) & 0 & 0 & 0 \\ 0 & 0 & 0 & G_{LR} & 0 & 0 \\ 0 & 0 & 0 & 0 & G_{LT} & 0 \\ 0 & 0 & 0 & 0 & 0 & G_{RT} \end{bmatrix}$

and $\Gamma = \dfrac{1}{1-\nu_{LR}\nu_{RL}-\nu_{RT}\nu_{TR}-\nu_{TL}\nu_{LT}-2\nu_{RL}\nu_{TR}\nu_{LT}}$

Hence, determining the engineering constants $\mathrm{E}, \nu, G$ are essentially required to define the properties of the adherent orthotropic material. Then, substituting using the above matrix formula to obtain the nine-material stiffness parameters $D_{ijkl}$ in normal, radial and tangential directions.

### 2.2 Modeling Approach of the glue-line

The glue-line performance could be expressed by a Cohesive Zone Model (CZM) to evaluate the progressive failure. The response of cohesive elements in numerical simulation may be based on a continuum description of the material (the actual interface thickness is being modeled), or on a traction-separation description of the interface (the interface thickness can be considered to be zero) which is the case in this study (Liu, 2006). Three-cohesive parameters characterizing the traction-separation relationship, the initial stiffness, damage initiation (described by the interface strength), and damage evolution (described by the interface fracture toughness $W$) need to be determined. The three-parameters could be determined using experimental techniques with appropriate analysis of standardized test. However, the fracture toughness (or the critical energy release rate) is still difficult to obtain. Therefore, it is available in literature or handbooks for many material systems (Liu, 2006; Sandhaas, 2012; Tran, Oudjene and Meausoone, 2014; Tran, Oudjene and Méausoone, 2015). For cohesive elements used to model bonded interfaces, the initial stiffness coefficient $(K_{nn}, K_{ss}, K_{tt})$ in normal, and two local shear directions respectively are required. That is defined as the ratio of traction vector stress to strain with the strain being defined as the ratio of separation $\delta$ to the initial constitutive thickness $T_0$, i.e. $(\varepsilon = \delta / T_0)$. In contrast with the most literature, the stiffness of cohesive elements $K'$ is defined as the ratio of traction-stress $t$ to separation-displacement $\delta$ (Liu, 2006; Dassault Systèmes Simulia, 2013). Thus,

$$K' = \frac{\bar{t}}{\delta} = \frac{\bar{t}}{\varepsilon . T_0} = \frac{K}{T_0}$$

The value of $K$ not $K'$ are required in the modeling process and both $K'\ and\ K$ are identical when the initial constitutive thickness $T_0$ is specified as 1.0. Therefore, the elasticity definition offered in Abaqus can be expressed directly in terms of the nominal tractions and nominal strains (Dassault Systèmes Simulia, 2013). Subsequently, to specify damage evolution, the value of fracture energy, and the critical cohesive strengths in the normal and the two local shear directions (Normal only, Shear-1 only, and Shear-2 only) are required. Hence, the initial stiffness $K$ can be expressed in a 3-D as follows:

$$t = \begin{Bmatrix} t_n \\ t_s \\ t_t \end{Bmatrix} = \begin{bmatrix} K_{nn} & K_{ns} & K_{nt} \\ K_{ns} & K_{ss} & K_{st} \\ K_{nt} & K_{st} & K_{tt} \end{bmatrix} \begin{Bmatrix} \varepsilon_n \\ \varepsilon_s \\ \varepsilon_t \end{Bmatrix} = \mathrm{K}.\varepsilon$$

Where $t_n, t_s, and\ t_t$ represent the nominal tractions in the normal and two local shear directions with respect to the crack plane, respectively; while $\varepsilon_n, \varepsilon_s, and\ \varepsilon_t$ are the corresponding nominal separation strains which defined respectively as $\varepsilon_n = \delta_n / T_0, \varepsilon_s = \delta_s / T_0, and\ \varepsilon_t = \delta_t / T_0$ being $\delta_n, \delta_s, and\ \delta_t$ as the separation-displacements between corresponding points at the interface, and $T_0$ is the constitutive thickness of the cohesive element (Fortino *et al.*, 2012; Dassault Systèmes Simulia, 2013). In this study, the off-diagonal stiffness terms are setting to zero for the uncoupled behavior between normal and two local shear components. Moreover, the same elastic properties where used for the two local shear directions for the cohesive element.

## 3 VERIFICATION FOR THE NUMERICAL FE MODEL

A verification strategy was followed to validate the Abaqus FEA model through comparing the numerical 3-D finite element load-displacement curves with experimental ones. The verification was divided into two parts according to timber and glue. The first part was to verify the model with the wood adherent properties which was spruce in this study. Then, second part was to verify the model with the glue properties which was here melamine-urea-formaldehyde (MUF) adhesive. A total of 3-specimens for each part were tested experimentally under four-point loading according to the standard test requirements of NLGA-SPS1. The ambient temperature was 20ºC at the time of the tests. The load was applied at a rate of 0.085 mm/sec. The deflection was measured with linear variable differential transformer (LVDT) placed at the mid-span of the specimen and recorded versus the applied load.

### 3.1 Verification for the timber

A total of 3-specimens of actual dry dimensions 38 x 89 x 1000 mm$^3$ were tested to measure the deflection using LVDT placed at the mid-span. The spruce mechanical properties data were identified based on standard tests which were performed and presented in (Fortino *et al.*, 2012; Sandhaas, 2012; Sandhaas and Van de Kuilen, 2013) where, the studies have specified approximately the same mechanical properties of spruce as orthotropic material in the longitudinal, radial, and tangential directions (see table 1).

Table 1 Mechanical Properties used for the analysis of the specimens

| $E_L$ | $E_R$ | $E_T$ | $G_{RL}$ | $G_{RT}$ | $G_{TL}$ | $\nu_{LR}$ | $\nu_{LT}$ | $\nu_{RT}$ | $\nu_{TR}$ | $\nu_{RL}$ | $\nu_{TL}$ |
|---|---|---|---|---|---|---|---|---|---|---|---|
| N/mm$^2$ | N/mm$^2$ | N/mm$^2$ | N/mm$^2$ | N/mm$^2$ | N/mm$^2$ | - | - | - | - | - | - |
| 11000 | 370 | 370 | 690 | 50 | 690 | 0.430 | 0.530 | 0.420 | 0.240 | 0.019 | 0.013 |

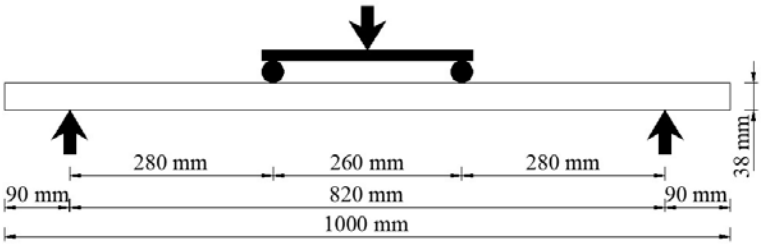


Figure 3 Schematic illustration of the specimen used in the test

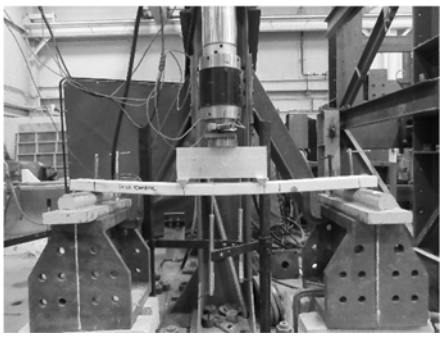

Figure 4 Typical experimental mode of spruce specimen without FJ

A model in Abaqus 6.14 was created by identifying the nine-independent stiffness parameters $D_{ijkl}$ using the specified mechanical properties of spruce. From substituting in the previous stiffness matrix we can get the nine-parameters as follows:

$$D_{ijkl}\,(MPa) = \begin{bmatrix} 9891.2 & 255.5901 & 259.3419 & 0 & 0 & 0 \\ 255.5901 & 367.4507 & 142.1542 & 0 & 0 & 0 \\ 259.3419 & 142.1542 & 366.9771 & 0 & 0 & 0 \\ 0 & 0 & 0 & 690 & 0 & 0 \\ 0 & 0 & 0 & 0 & 690 & 0 \\ 0 & 0 & 0 & 0 & 0 & 50 \end{bmatrix}$$

Therefore, these data are directly required to define the spruce mechanical properties in Abaqus software.

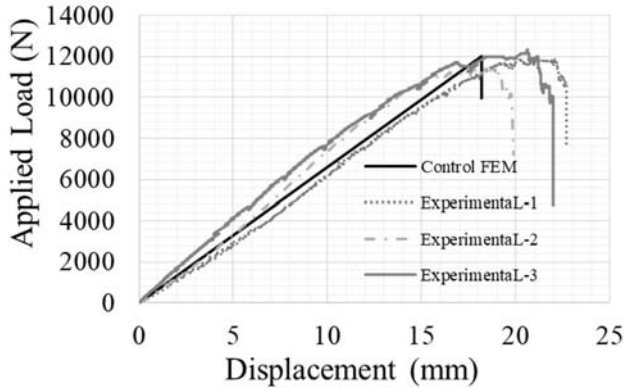


Figure 5 Comparison between experimental and numerical load-displacement curves for spruce specimen without FJ

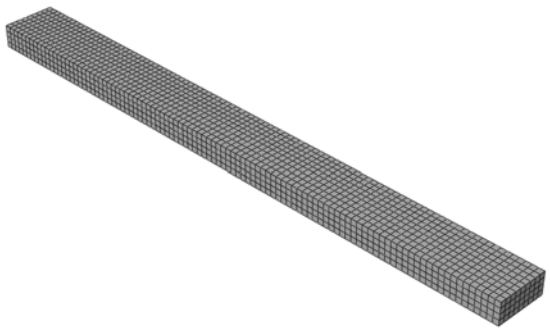

Figure 6 Finite Element model of the specimen without FJ

Figure 5 showed the load-displacement curves for the 3-specimens and for the finite element model to make a comparison between experimental data and numerical model data. The curves showed a close agreement between both data which validate the model for the spruce properties.

### 3.2 Verification for the glue

A total of 3-specimens with FJ of actual dry dimensions 38 x 89 x 1000 $mm^3$ were tested to measure the deflection to validate the numerical 3-D finite element FJ model. Each specimen consists of one-FJ at the mid-span in which, the FJ length was 28.27 mm, the pitch was 6.33 mm, and the finger-tip width (tip thickness) was 0.76 mm. FJs were assembled with a one face glue using melamine-urea-formaldehyde

(MUF) adhesive of constitutive thickness $T_0 = 0.3mm$. The FJ pieces were pressed at 20º C with a constant end pressure for 24 hours. Then, the specimens were tested after 24 hours of curing at room temperature. The MUF properties data were identified based on standard tests for mode I (DCB test) and mode II, III (shear test) which were performed and presented in (Fortino *et al.*, 2012; Tran, Oudjene and Meausoone, 2014; Tran, Oudjene and Méausoone, 2015) (see table 2).

Table 2 Melamine-Urea-Formaldehyde (MUF) adhesive properties used for mode I, II, and III

| | | |
|---|---|---|
| Mode I | Normal Stiffness $K_{nn}\ (N/mm^2)$ | Normal Strength $\sigma_{nn}\ (N/mm^2)$ |
| | 1.35 | 1.6 |
| Mode II | Shear-1 Stiffness $K_{ss}\ (N/mm^2)$ | Shear-1 strength $\sigma_{ss}\ (N/mm^2)$ |
| | 9 | 9.7 |
| Mode III | Shear-2 Stiffness $K_{tt}\ (N/mm^2)$ | Shear-2 strength $\sigma_{tt}\ (N/mm^2)$ |
| | 9 | 9.7 |

Also, the initial stiffness $K$ used in this study can be represented in the following matrix:

$$t = \begin{bmatrix} 1.35 & 0 & 0 \\ 0 & 9 & 0 \\ 0 & 0 & 9 \end{bmatrix} \varepsilon$$

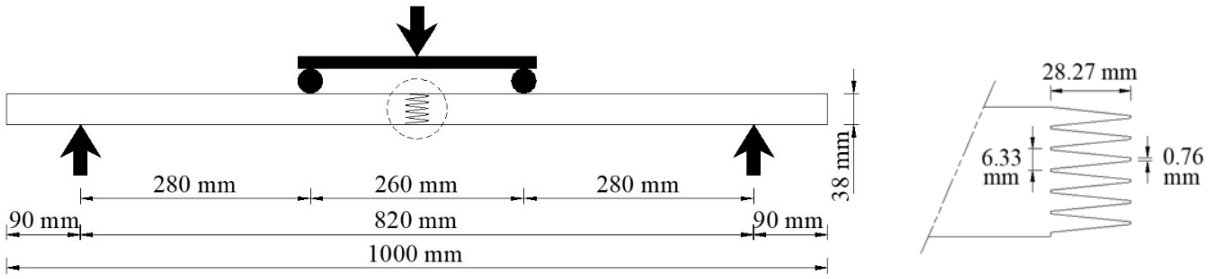


Figure 7 Schematic illustration of the specimen with FJ at mid-span

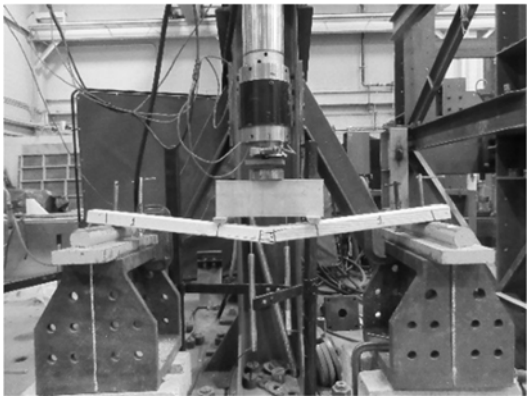

Figure 8 Experimental failure of specimen with FJ

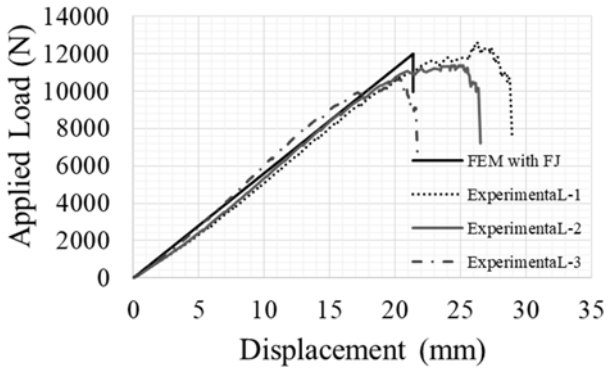


Figure 9 Comparison between experimental and numerical load-displacement curves for spruce specimen with FJ

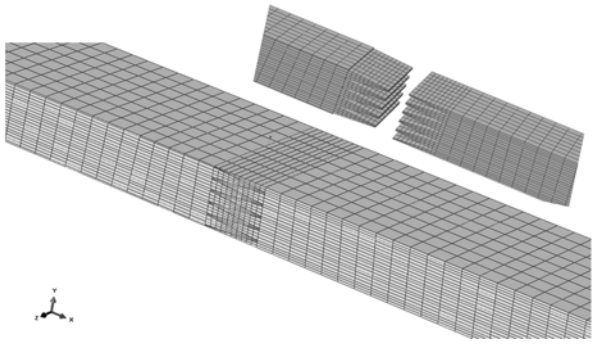

Figure 10 Finite Element model of the specimen with FJ

The load-displacement curves in figure 8 showed a close agreement between both experimental and numerical model data which validate the model for adhesive properties with the spruce adherent used.

## 4 CONCLUSION

In this study, the objective was to create a numerical 3-D finite element model using Abaqus FEA software to simulate structural finger-joined spruce wood lumber. The created numerical model was based on cohesive zone model (CZM) using traction-separation law relationship to model the interface between the two timber parts. The properties of wood (adherent part) and glue (adhesive part) were specified to be used in the finite element model to simulate the FJ lumber. The spruce wood properties comprised of 3-young's moduli, 6-poisson's ratios, and 3-shear moduli. Whereas, the glue-line properties were the initial stiffness, damage initiation (described by the interface strength), and damage evolution (described by the interface critical energy release rate) in a Mixed-Mode behaviour. The numerical load-displacement curve were then calculated to be compared with the experimental curve to validate the developed model. The results showed that the load-displacement curves were in a close agreement between the experimental and numerical model data which validate the developed model for the MUF adhesive properties with the spruce adherent used.

The Simulation of the FJ lumber using numerical 3-D FEM provide a valuable resource for performing engineering analysis. The numerical FEA model will be useful to determine the stiffness of FJ lumber directly, which affects both modulus of elasticity and modulus of rupture, without the need to waste a piece of lumber in an experiment to specify the stiffness. In addition, the FJ numerical FEA model can be used to make timber design useful and easy for structural applications such as: structural glulam beam, column, curved and arched members. Modeling of FJ using FEA will improve the understanding of the structural behaviour and lead to a great potential for wider structural applications. This will enable the engineering wood industry to produce a larger variety of the pieces of wood that are being fabricated with preferred structural performance.

Eventually, numerical FEA models could be used as a tool in enhancing the existing FJ techniques which play a major role in exploiting the unused and inexpensive wasted short wood pieces which harm the environment. FJ can extend the scraps by joining them together end to end to make a valuable longer piece. Hence FJ will contribute to protecting the environment through the efficient exploitation of every timber piece of the tree.

**References**


Dassault Systèmes Simulia (2013) 'Abaqus CAE User's Manual'.

Fortino, S. *et al.* (2012) 'A simple approach for FEM simulation of Mode I cohesive crack growth in glued laminated timber under short-term loading', *Rakenteiden Mekaniikka (Journal of Structural Mechanics)*, 45(1), pp. 1–20.

Holmberg, S., Persson, K. and Petersson, H. (1999) 'Nonlinear mechanical behaviour and analysis of wood and fibre materials', *Computers & Structures*, 72(4–5), pp. 459–480. doi: 10.1016/S0045-7949(98)00331-9.

Jokerst, R. W. (1981) 'Finger-Jointed Wood Products', *US Forest Service*, (April).

Liu, C. (2006) 'Selecting Material Parameters in Abaqus for Cohesive Elements Defined in Terms Of Traction-Separation', *Mechanical Engineering*, pp. 1–2.

NLGA-SPS-1 (2014) 'Special Products Standards for Finger-Joined Structural Lumber', *National Lumber Grades Authority*.

Sandhaas, C. (2012) *Mechanical Behaviour of Timber Joints With Slotted-in Steel Plates*.

Sandhaas, C. and Van de Kuilen, J. W. G. (2013) 'Material Model for Wood', 58(2), pp. 179–200.

Tollefson, J. (2017) 'The wooden skyscrapers that could help to cool the planet', *Nature*, 545(7654), pp. 280–282. doi: 10.1038/545280a.

Tran, V. D., Oudjene, M. and Meausoone, P. J. (2014) 'FE analysis and geometrical optimization of timber beech finger-joint under bending test', *International Journal of Adhesion and Adhesives*. Elsevier, 52, pp. 40–47. doi: 10.1016/j.ijadhadh.2014.03.007.

Tran, V., Oudjene, M. and Méausoone, P. (2015) 'Experimental and numerical analyses of the structural response of adhesively reconstituted beech timber beams', *COMPOSITE STRUCTURE*. Elsevier Ltd, 119, pp. 206–217. doi: 10.1016/j.compstruct.2014.08.013.